Surface & Coatings Technology 204 (2010) 1493–1502

Contents lists available at ScienceDirect

Surface & Coatings Technology

journal homepage: www.elsevier.com/locate/surfcoat

Optimization of carbon doped molybdenum oxide thin film coating process using designed experiments

Charnnarong Saikaew [a,*], Anurat Wisitsoraat [b], Rangsrit Sootticoon [a]

[a] Department of Industrial Engineering, Khon Kaen University, Khon Kaen, Thailand
[b] National Electronics and Computer Technology Center, 112 Pahol Yothin Rd., Pathumthani, Thailand

ARTICLE INFO

Article history:
Received 25 June 2009
Accepted in revised form 29 September 2009
Available online 8 October 2009

Keywords:
Carbon doped molybdenum oxide
Sputtering process
Central composite design
Response surface analysis
Desirability function

ABSTRACT

In this work, central composite design (CCD) is applied to study carbon doped MoO_x thin film deposition by sputtering process. The CCD based experimental study is made by varying four controllable input process factors including radio frequency (r.f.) power, operating pressure, argon to oxygen flow ratio, and carbon doping gas to oxygen flow ratio and output responses are deposition rate and surface roughness. Response surface methodology (RSM) with desirability function is used to determine an optimum sputtering condition that simultaneously maximizes the deposition rate and surface roughness of carbon doped MoO_x thin film coating. Empirical models derived from regression analyses for deposition rate and surface roughness are found to be second order functions of these four process factors. From RSM analysis with desirability function, the optimal operating condition for carbon doped MoO_x thin film coating that produces a maximum deposition rate of 8.4 nm/min and a maximum surface roughness of 41.7 nm is obtained at r.f. power of 150 W, operating pressure of 0.8 Pa, argon to oxygen flow ratio of 0.59, and carbon doping gas flow ratio of 0.08 with the overall desirability of 64%.

1. Introduction

Molybdenum oxide (MoO_x) is an interesting material for a number of applications including catalysts, chemical sensors, and energy storage devices [1–5]. The most basic and stable structure of MoO_x is in an orthorhombic form. It has low density and low melting point of ~800 °C. In addition, it is an n-type semiconductor with a bulk band gap of ~3.2 eV and its sheet resistivity is in the order of $10^{10}\,\Omega\,m$ at room temperature. At elevated temperatures above 250 °C, MoO_x material becomes highly reactive because it will be readily reduced by any reducing gases. MoO_x is catalyst for NO_2 to NO conversion. In addition, MoO_x has been studied as an active element for gas sensing applications and it was found to be very sensitive to various gases such as NO, NO_2, CO, H_2, and NH_3 [6–8].

Several fabrication techniques for MoO_x thin film coating such as thermal evaporation, sputtering, chemical vapor deposition (CVD), spray pyrolysis, have been studied. Among them, sputtering technique is the most widely employed because of high quality, well controlled process, and integrated circuit (IC) compatibility. Foreign atom addition into thin film structure is an effective mean to improve material properties and functionality. Thus far there have been few reports involving incorporation of foreign atom into MoO_x thin films and nanostructures. Recently, the introduction of carbon dopant by gas source is employed to modify various properties of MoO_x nanostructure thin film [9]. This is a potential mean for improving MoO_x thin film material due to simplicity and low cost. However, the reported carbon doped MoO_x thin film sputtering study was performed by considering only the effect of carbon doping gas concentration by keeping all other factors in the experiment fixed. This type of experiment is called *one-factor-at-a-time experimentation approach*. Note that one-factor-at-a-time experiment consists of selecting a starting point or baseline set of levels for each factor, then successively varying each factor over its range with the other factors held constant at the baseline level [11]. This one-factor-at-a-time approach cannot give comprehensive understanding for real physical system because the interactions among factors cannot be analyzed. This common technique requires large resources to obtain a limited amount of information about the process. Furthermore, it is unreliable, inefficient, time consuming, and might yield false optimum settings for the process. For commercial and industrial applications, it is important to comprehensively understand the role of deposition factors on the coating characteristics of the thin film.

Design of experiments (DOE) is a systematic approach that can be used to efficiently study the roles of multiple experimental factors on any output characteristics of a process. In addition, it can be used to control, predict, and optimize a complex process for any desire behaviors. Design of experiments plays a major role in manufacturing process development, a new product design, and process improvement. DOE is also used to develop a process affected minimally by external sources of variability. Furthermore, it is a rigorous method for both achieving desired properties and determining an optimized mixture.

* Corresponding author. Tel./fax: +66 43 343 117.
E-mail address: charn_sa@kku.ac.th (C. Saikaew).

0257-8972/$ – see front matter © 2009 Elsevier B.V. All rights reserved.
doi:10.1016/j.surfcoat.2009.09.083

Central composite design (CCD) is one of the most widely employed DOE techniques. CCD is a popular design suitable for fitting a second-order model, which is applicable for several physical processes including thin film deposition [10]. Generally, the CCD consists of a 2^k factorial runs with $2k$ axial or star runs and 3 to 5 center runs, where k denotes number of factors [11]. The response from DOE can be systematically analyzed to yield process model and optimization by various statistical methodologies. Response surface methodology (RSM) is one of the most widely used statistical methodologies for DOE because it can be used to obtain optimal operating conditions of statistically significant factors for most general processes.

RSM, by definition, is "a collection of mathematical and statistical techniques that are useful for the modeling and analysis of problems in which a response of interest is influenced by several factors and the objective is to optimize this response" [11]. Many response surface problems involve the analysis of multi-response variables. Simultaneous consideration of multi-response variables is to build an appropriate response surface model for each response variable and try to obtain a set of operating conditions that optimizes all response variables or keeps them in desired ranges. Many numerical techniques can be used to solve a simultaneous optimization problem [11]. One of the most useful techniques to simultaneous optimization of multi-response variables is the use of desirability functions presented by Derringer and Suich [12].

The general approach is to convert each response variable, y_i into an individual desirability function that varies over the range from 0 to 1 (least to most desirable, respectively). To transform each response variable into an individual desirability function, three cases of objective function arise: maximization, minimization, and meeting a target [13]. For maximization, the objective function increases from 0 to 1 as input factor increases from low to high value. It is reverse for minimization and the function to meet the target is the combination of desirability functions for the goal of maximization and minimization. After obtaining the individual desirability function for each objective function, the overall desirability is calculated to determine the best combination of responses. For the overall desirability, D, the equation is:

$$D = \left(\prod_{i=1}^{n} d_i\right)^{1/n} \quad (1)$$

where d_i represents the desirability of each individual response and n is the number of responses being optimized. If one of the response variables is unacceptable (i.e., $d_i = 0$), the overall desirability, D, is unacceptable (i.e., $D = 0$). The overall desirability function must be maximized to obtain the optimal operating conditions. The goal seeking begins at a random starting point and proceeds up the steepest slope to a maximum. There may be two or more maximums because of curvature in the response surfaces and their combination into the desirability function. By starting from many points in the design space, chances improve for obtaining the best local maximum.

DOE approach using CCD and RSM have been applied for studying and optimizing various sputtered thin film materials such as lead zirconium titanate [15], aluminum nitride [16,17], yttrium aluminum garnet [18]. However, there has been no systematic investigation of sputtered molybdenum oxide thin film coating using. DOE approach. In this work, CCD is applied to study carbon doped MoO_x thin film deposition by sputtering process. The CCD based experimental study was made by varying four controllable input parameters including radio r.f. power, operating pressure, argon to oxygen flow ratio and carbon doping gas to oxygen flow ratio and output responses are deposition rate and surface roughness. The objective is to understand the roles of these parameters on carbon doped MoO_x thin film coating and optimize deposition rate and surface roughness characteristics for potential applications. Response surface methodology (RSM) with desirability function is used to quantitatively analyze the experimental data along with qualitative material analysis based on scanning electron microscopy.

2. Research methodology

In this work, a seven-step approach involved planning and conducting the experiment is described as follows:

1. *Setting the objective*: The main objective is to obtain the optimal operating conditions of process factors of thin film deposition for determination the maximum deposition rate and surface roughness in thin film deposition process of gas sensor fabrication. High deposition rate is preferred to increase throughput for commercial production while maximized surface roughness would enhance gas sensing sensitivity of MoO_x based gas sensor.
2. *Identifying the important process factors*: From carbon doped MoO_x thin film sputtering process consideration, there are four main parameters that control the coating behaviors including r.f. power, pressure, carbon doping gas to oxygen flow ratio and argon to oxygen flow ratio. Acetylene is selected as carbon doping gas for molybdenum oxide thin film coating due to low cost. These four controllable parameters are chosen because they are the main factors for sputtering process and they are not machine or system dependent. It should be noted that there are still additional process factors that can influence the MoO_x thin film sputtering process. These include substrate temperature, external dc bias at the substrate, sample to target spacing and magnetic field at sputtering head. Additional heater for substrate is required to control substrate temperature. For external dc bias, extra dc power supply with r.f.-compatibility is needed. To vary sample to target spacing and magnetic field at sputtering head, machine modifications are needed. These machine and system dependent parameters are thus excluded from this study.
3. *Determining the upper and lower limits of the process parameters*: For the present sputtering system, the range of r.f. power, pressure, argon to oxygen flow ratio and carbon doping gas to oxygen flow ratio are 50 to 250 W, 0.2 Pa to 1.0 Pa, 0/100 to 50/50 and 0/100 to 30/70, respectively. The range of r.f. power is determined from the constraint of sputtering machine, which use magnetron sputter head with 3″ target while this range of pressure is suitable for r.f. plasma operation. The range of argon to oxygen flow ratio is defined for molybdenum oxide formation. If this ratio is higher than 50/50, molybdenum will be partial oxide or metallic. The range of acetylene–oxygen flow ratio is limited to 30/70 so that carbon content is not excessive and material becomes partial carbide.
4. *Developing of the design matrix based on CCD*: The CCD for this study consists of a 2^4 factorial runs with 8 axial or star runs and 6 center runs. The list of experiments designed based on CCD is shown in Table 1.
5. *Conducting the deposition of carbon doped MoO_x thin film as per the design matrix*: The carbon doped MoO_x thin film was deposited using a magnetron sputtering system. This system consists of a high vacuum chamber equipped with a 3″ target magnetron gun, 600 W radio frequency generator, 400 W DC power supply and a turbomolecular pump. The molybdenum oxide was deposited on a (100) silicon substrate through an electroplated shadow mask with a 400 μm × 800 μm rectangular pattern by reactive sputtering of pure molybdenum target under a mixture of argon (Ar), oxygen (O_2) and acetylene (C_2H_2) gases. Carbon doped MoO_x thin film depositions were then systematically performed according to CCD as listed in Table 1. There were five samples for each condition and the experiments were run in random order to avoid a statistical bias in the analyses.
6. *Recording responses*: The film thickness and surface roughness of the film were measured by white-light interferometric optical profiler (Polytech model 2000). The deposition rate response is then calculated from the film thickness and deposition time. In addition, the surface morphology, microstructure, and chemical composition of metal oxide thin films were examined by means of scanning electron microscope (SEM) and energy dispersive X-ray

Table 1
List of CCD experiments along with average deposition rate and surface roughness responses.

Trial no.	R.f. power (W)	Pressure (Pa)	Ar/O_2	C_2H_2/O_2	Average deposition rate (nm/min)	Average surface roughness (nm)
1	100	0.4	20/80	5/95	3.59	36.4
2	100	0.4	20/80	20/80	4.50	30.6
3	100	0.4	40/60	5/95	2.93	53.3
4	100	0.4	40/60	20/80	5.47	37.0
5	100	0.8	20/80	5/95	3.13	46.7
6	100	0.8	20/80	20/80	3.68	40.8
7	100	0.8	40/60	5/95	3.68	49.3
8	100	0.8	40/60	20/80	4.68	38.2
9	200	0.4	20/80	5/95	9.17	35.1
10	200	0.4	20/80	20/80	14.64	29.6
11	200	0.4	40/60	5/95	6.92	43.9
12	200	0.4	40/60	20/80	11.99	27.0
13	200	0.8	20/80	5/95	6.55	42.2
14	200	0.8	20/80	20/80	13.18	33.2
15	200	0.8	40/60	5/95	10.30	37.1
16	200	0.8	40/60	20/80	14.71	29.2
17	150	0.6	25/75	10/90	8.43	40.2
18	150	0.6	25/75	10/90	8.32	39.6
19	150	0.6	25/75	10/90	8.55	37.6
20	150	0.6	25/75	10/90	8.27	40.6
21	150	0.6	25/75	10/90	8.64	39.7
22	150	0.6	25/75	10/90	8.34	40.9
23	50	0.6	25/75	10/90	0.80	25.4
24	250	0.6	25/75	10/90	12.64	26.1
25	150	0.2	25/75	10/90	8.72	36.3
26	150	1.0	25/75	10/90	7.72	40.5
27	150	0.6	0/100	10/90	3.85	45.1
28	150	0.6	50/50	10/90	8.03	35.0
29	150	0.6	25/75	0/100	5.43	41.9
30	150	0.6	25/75	30/70	9.05	42.1

spectroscopy (EDX). SEM and EDX measurements (Hitachi model S-3400N) were performed in secondary electron mode at an accelerating voltage of 20 kV. The elemental compositions were calculated by EDX's analysis software (ISIS ver. 3.3 by Oxford Instrument) based on Cliff–Lorimer ratio method.

7. *Determining the optimum operating conditions for the system using response surface methodology (RSM) with desirability function*: The objectives of this analysis are to maximize both the deposition rate and surface roughness. Thus, two individual desirability functions are needed. The implementation of the two individual desirability functions and the optimization was conducted using the Design-Expert® V7 software package. This software package provides a three-dimensional plot of the response surface and a two-dimensional plot of the contour for each response variable and overall desirability versus selected process factors. Design-Expert® uses an optimization method developed by Derringer and Suich [12] described by Myers and Montgomery [11].

3. Experimental results

The characteristics of the molybdenum oxide thin film coating are characterized quantitatively in terms of deposition rate and surface roughness of deposited films at a constant average film thickness of 300 nm. Along with the quantitative analysis, qualitative SEM and EDX results will be discussed to explain related structural effects including surface morphology and chemical compositions. Typical 3-dimensional and cross-section profiles of sputtered molybdenum oxide thin film from interferometric measurement are shown in Fig. 1(a) and (b), respectively.

The profile analyses give the average film thickness of 275.2 nm and the root mean square (r.m.s.) surface roughness of 57.2 nm. This film is one sample that was deposited under the growth conditions trial no. 3 and deposition time is 90 min. The deposition rate of 3.06 nm/min is thus obtained. The complete results of average deposition rate and corresponding surface roughness for all experimental conditions are listed along with CCD experiment parameters in Table 1.

To determine the optimal operating conditions of the significant process factors influencing deposition rate and surface roughness in thin film deposition of gas sensor, a numerical analysis using response surface methodology is carried out. Two different quality characteristics are initially targeted for optimization. After performing regression analysis, an empirical relationship between the deposition rate and the r.f. power, operating pressure, argon to oxygen flow ratio, and carbon doping gas to oxygen flow ratio is

$$\hat{y}_1 = 9.22 + 3.45A + 0.085B + 0.43C + 1.59D + 1.05AD + 0.69BC - 0.47A^2 - 0.45C^2 - 0.58D^2 \quad (2)$$

where $\hat{y}_1$ is the deposition rate response variable whereas A, B, C, and D are r.f. power, operating pressure, argon to oxygen flow ratio, and carbon doping gas to oxygen flow ratio, respectively. The predictive model of deposition rate is derived based on the sequential model sum of squares analysis. The sequential model sum of squares has been used to determine whether linear terms, two-factor interactions or quadratic source of terms should be added to a predictive model [13]. Based on the sequential model sum of squares analysis, linear terms and two-factor interactions are not sufficient (p-value>0.05). However, if quadratic terms are added, the model shows statistically significant (p-value<0.05). Hence the predictive model of deposition rate includes the two-factor interactions terms and the quadratic terms as shown in Eq. (2). Analysis of residuals shows no serious anomalies with the model assumptions of normality, independence, and constant variance of the observations. The goodness of fit of the model is checked by determination coefficient (R^2). The coefficient of determination provides the proportion of the total variation in the response variable explained by the process factors included in the model [11]. The adjusted determination coefficient (adjusted R^2) is a measure of the amount of variation around the mean explained by the model, adjusted for the number of terms in the model. As the number of terms in the model increases, the adjusted R^2 decreases because those additional terms do not add value to the model. The high value of R^2 indicates that the model adequately explains the carbon doped MoO_x thin film deposition process. From the analysis of variance (ANOVA), the value of determination coefficient ($R^2 = 95\%$) indicates that only 5% of the total variations are not explained by the model. The value of adjusted determination coefficient (adjusted $R^2 = 93\%$) is also very high to advocate for a high significance of the model. The overall model is statistically significant. Thus, the predictive model shows a good fit.

From the regression model and ANOVA analyses, r.f. power (A) and carbon doping gas to oxygen flow ratio (D) are found to have significant effects on deposition rate while operating pressure (B) and argon to oxygen flow ratio (C) have less and least impacts on the response, respectively. It can be seen that the coefficient of interaction term, AD, is comparable to linear terms. Thus, interaction between r.f. power and carbon doping gas to oxygen flow ratio (AD) has also significant effect on deposition rate. However, interaction between operating pressure and argon to oxygen flow ratio (BC) has relatively low impact on the response.

In order to visualize the dependence of deposition rate on process factors, contour and surface plot can be constructed using Eq. (2). Fig. 2 shows a contour plot and a response surface plot for the deposition rate response in terms of two significant process factors, r.f. power and carbon doping gas to oxygen flow ratio while other process factors are maintained at their middle values. The plots reveal that the amount of r.f. power makes higher impact than the amount of carbon doping gas to oxygen flow ratio on the response. Furthermore, the

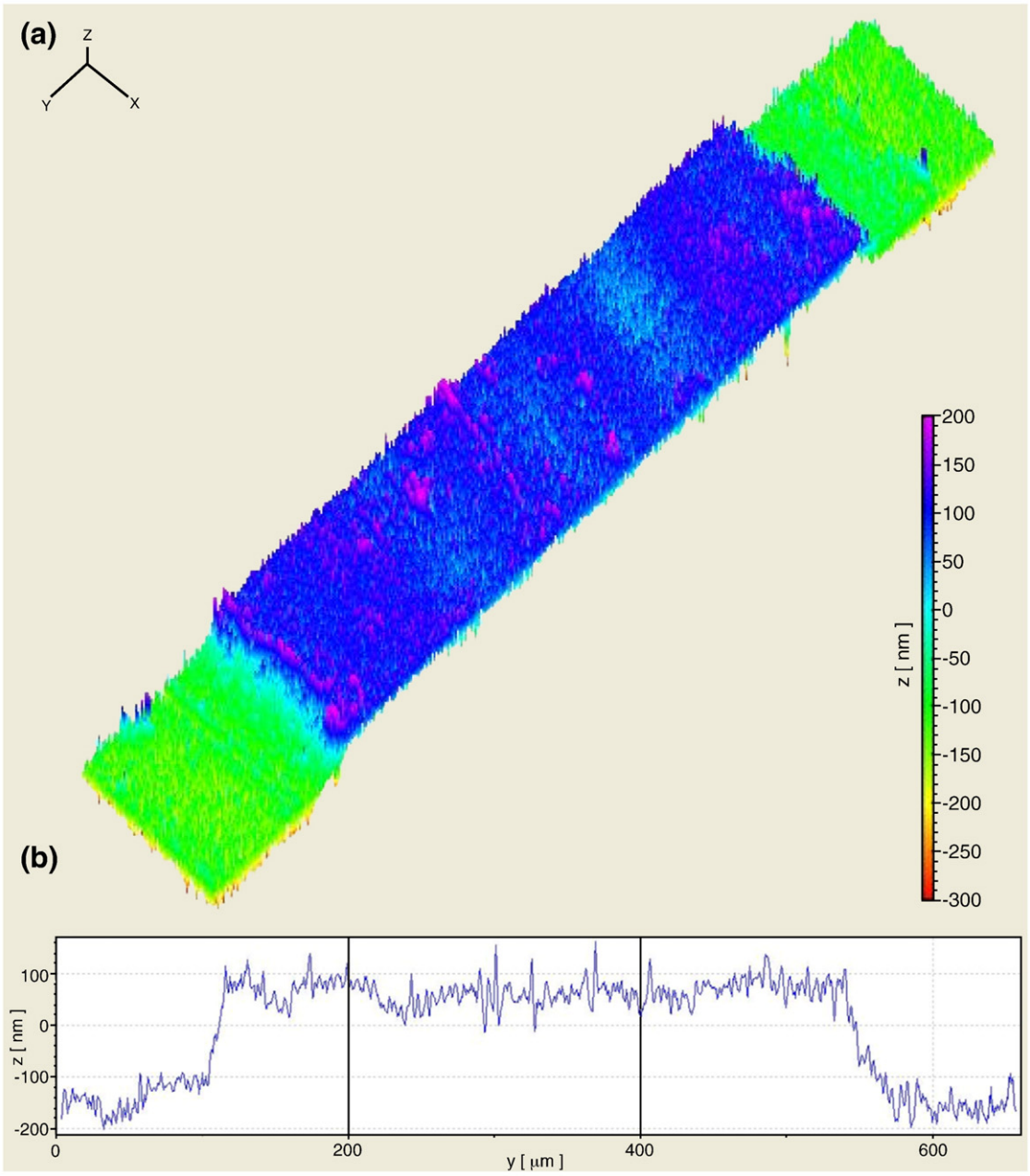

Fig. 1. Typical (a) 3-dimensional and (b) cross-section profile of sputtered molybdenum oxide thin film from interferometric measurement.

deposition rate increases in the region of high r.f. power and carbon doping gas to oxygen flow ratio. This means that simultaneous increase of both factors brings about deposition rate increase. This is a result of a positive sign for the coefficient of interaction between r.f. power and carbon doping gas to oxygen flow ratio (*AD*). This is also confirmed when considering the sign for coefficients in the fitted model. The positive signs for the coefficients in the fitted model for deposition rate indicate that the amount of deposition rate increases with increasing levels of the four process factors, especially r.f. power and carbon doping gas to oxygen flow ratio.

The results from quantitative effect analyses on deposition rate can be explained by considering the principle of sputtering process. It is not surprising that r.f power directly increases the deposition rate because more ions with higher energies are impinging on the cathode generating more neutral sputtered atoms and electrons as the plasma voltage (between the anode and the cathode) is increased when r.f power increased. However, the considerable increase of deposition rate due to carbon doping gas to oxygen flow ratio is not initially anticipated. This effect may be explained after consideration of reactive chemical reaction between acetylene and oxygen gases occurs during this reactive sputtering. The dominant combustive reaction is given by [14]:

$$C_2H_2 + O^- \longrightarrow 2C(s) + H_2O + e^- + \text{Heat energy} \qquad (3)$$

The heat energy is mainly occurred in the plasma and it can partly be transferred to substrate via radiation, diffusion and conduction. The heat energy can be carried by all products in the plasma and the amount that it can carry is depending on its specific heat. Argon ions are expected to carry significant portion of heat energy because they have relatively larger size compared to other products. Thus, the deposition rate should be increased due to the effect of additional heat energy that can increase the energy of argon and oxygen ions, enhancing sputtering and oxidation rate of molybdenum. The interaction between r.f. power and acetylene to

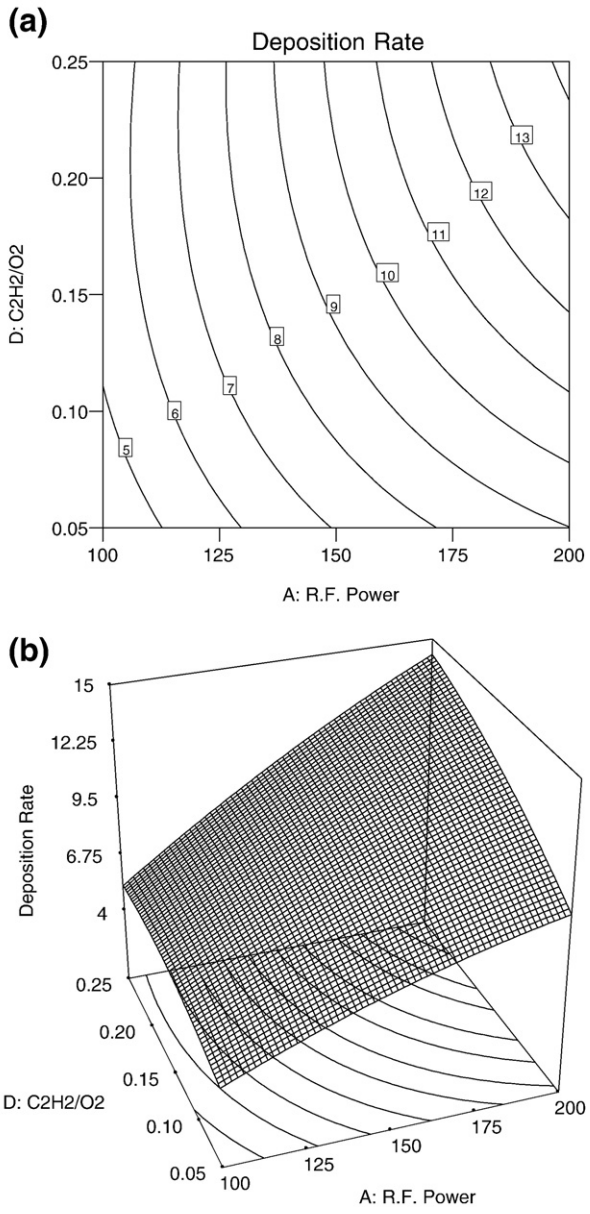

Fig. 2. (a) Contour plot and (b) response surface plot of deposition rate.

oxygen flow ratio can also be understood based on this reaction. From Eq. (3), the rate of reaction will increase with acetylene gas and oxygen ion, which will be increased as r.f. power increased.

The value of generated heat energy for this reaction is greater than 209 kJ/mol, which is corresponding to 50 kcal/mol. This is inferred from similar combustion reaction between oxygen and acetylene [23]. The heat power can then be calculated at a given acetylene flow rate using acetylene density (~1.1 kg/m^3) and molecular weight (26). At acetylene flow rate of 100 sccm (cm^3/min) (trial#30), the heat power is estimated to be ~15.3 W, which is more than 10% of the sputtering power. Thus, the increase of heat energy due this reaction is considerable and it should be a key mechanism responsible for linear and interaction dependence of deposition rate on acetylene to oxygen flow ratio and sputtering power as seen in Eq. (3). Moreover, additional electrons due to the reaction in Eq. (3) and corresponding increased secondary electrons at the cathode surface can also contribute to higher sputtering rate by enhancing energetic ionization.

Carbon doping into molybdenum oxide can also be directly depicted from Eq. (3). Similar to deposition rate, carbon doping concentration should also be increased with r.f. power and acetylene to oxygen flow ratio. The carbon doping in molybdenum oxide has been confirmed by EDX measurement. The effect of r.f. power on carbon doping is illustrated in EDX spectra as shown Fig. 3(a) and (b). It should be noted that the difference of carbon contents between EDX spectra are difficult to visualize because the amplitudes of carbon peaks are much smaller than those of oxygen and molybdenum. However, the inset elemental composition table shows that carbon contents are relatively large. This can be explained by considering the details of EDX analysis. In the analysis, the peak amplitudes corresponding to X-ray emission of all existing elements are calculated from measured EDX spectra. Each peak value will be corrected by scattering factor of each element. The scattering factor value is decreased nonlinearly with atomic weight of each element. The scattering factor of carbon is larger than that of oxygen and much larger than that of molybdenum. From the inset tables in Fig. 3, it is evident that the carbon content of molybdenum oxide thin film is considerably increased from ~5% to ~16% as r.f. power is doubled from 100 W to 200 W. Thus, the result is in agreement with mechanism explaining deposition rate. For both runs, operating pressure, argon to oxygen flow ratio and carbon doping gas to oxygen flow ratio are fixed at 0.6 Pa, 20/80 and 20/80, respectively. Similar results were observed for other pairs of runs with different r.f. powers.

The effect of acetylene to oxygen flow ratio on carbon doping is demonstrated in EDX spectra as shown Fig. 4(c) and (d). It is obvious that the carbon content of molybdenum oxide thin film is significantly increased from ~4% to ~30% as acetylene to oxygen flow ratio is increased from 0:100 (undoped) to 30:70. Thus, the result confirms the carbon doping due to acetylene gas. For both runs, r.f. power, operating pressure and argon to oxygen flow ratio are fixed at 150 W, 0.6 Pa and 25/75, respectively. Similar results were confirmed for other pairs of runs with different carbon doping gas to oxygen flow ratios. It should be noted that undoped molybdenum oxide thin film is indicated to have carbon content of ~4% because EDX measurement cannot give accurate carbon content due to carbon contamination in SEM system. As a result, carbon contents of the films by EDX measurement cannot be used for quantitative analysis.

Moreover, oxygen composition (x) of the MoO_x film calculated from the EDX data is found to be in the range from 6 to 9. This is more than twice of expected value of 3 for MoO_3 structure. Thus, EDX measurement also gives very inaccurate oxygen content. The main cause of the error is that the film thickness (~300 nm) is much smaller than electron penetration depth (~3 μm) at 20 keV. Since the film is thin, electrons are largely scattered with the silicon substrate and X-ray emitted from Si atoms can cause additional emitted X-ray from elements lighter than Si. Although EDX technique cannot provide accurate composition of thin film, it is still useful for qualitative comparison of composition of thin film.

Similar analyses are repeated for responses y_2 (surface roughness). The model for predicting average surface roughness is

$$\hat{y}_2 = 38.25 - 2.66A + 0.93B + 0.2C - 3.97D - 2.1AC - 2.08BC - 3.07A^2 + 1.9D^2 \quad (4)$$

Based on the sequential model sum of squares analysis, linear terms and two-factor interactions are not sufficient (p-value>0.05). However, if quadratic terms are added, the model becomes statistically significant (p-value<0.05). Hence the predictive model of surface roughness includes the two-factor interactions terms and the quadratic terms as shown in Eq. (4). The value of determination coefficient (R^2) and the value of adjusted determination coefficient (adjusted R^2) are acceptable and close to each other at 76% and 66%, respectively. The residual analysis for this model is satisfactory. It should be noted that the model is not fitted with the highest possible value of R^2 because a larger value of R^2 does not necessarily imply that the regression model is a good one [11]. In general, R^2 increases as we add terms to the model but some added terms may be statistically insignificant. An adjusted R^2 is used to

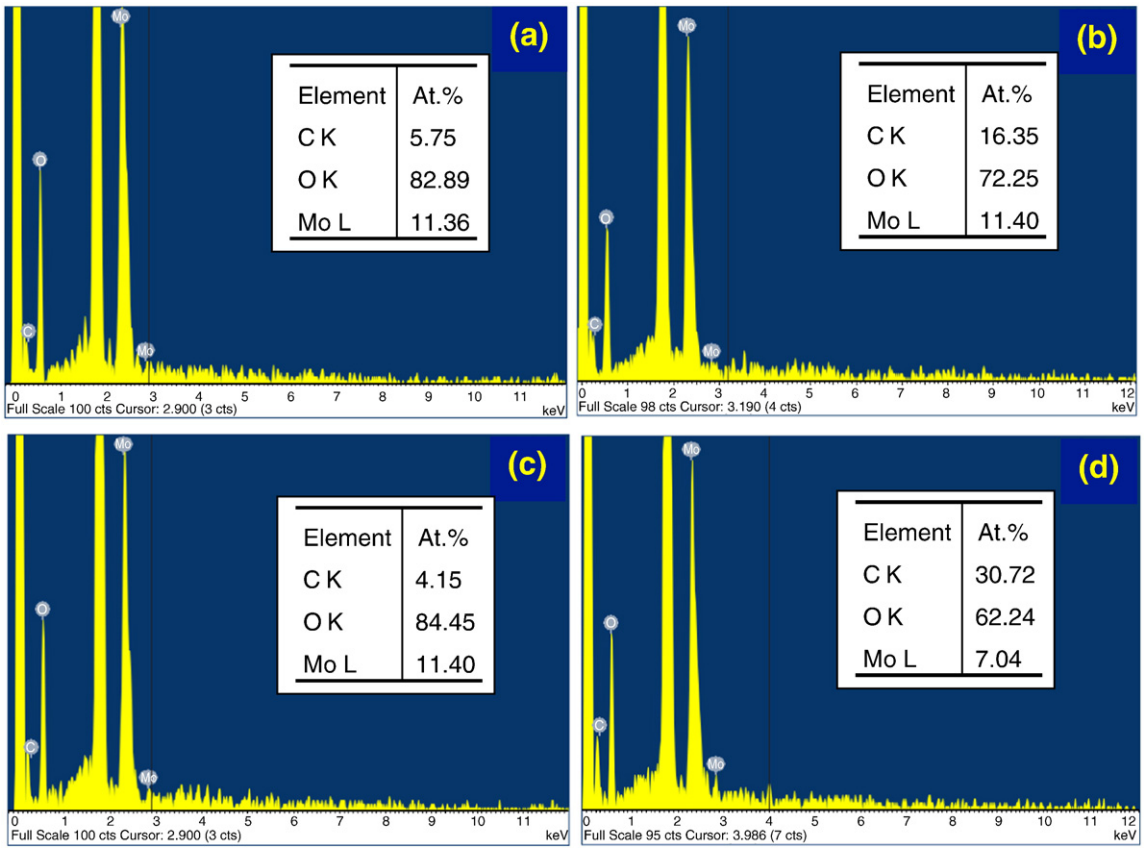

Fig. 3. EDX spectra of molybdenum oxide thin films (a) trial#2 (low r.f. power of 100 W) (b) trial#10 (high r.f. power of 200 W) (c) trial#29 (low acetylene to oxygen flow ratio of 0:100) and (d) trial#30 (high acetylene to oxygen flow ratio of 30:70).

identify whether the added terms are necessary. If unnecessary terms are added, the value of adjusted R^2 will often decrease. Thus, when R^2 is very close to the adjusted R^2, it means that significant terms have already been included in the model. For the present model, the adjusted R^2 will decrease and significantly different from R^2, if additional factors are added. Thus, the model is statistically appropriate. Although the R^2 value of 76% is considered quite low, it is generally acceptable (for example see [19,20]). The low R^2 may be the results of large response variation for a random process, which may be unavoidable in some cases. This can be the case for surface roughness because of its partly random nature.

From the regression model and ANOVA analysis, r.f. power (A) and carbon doping gas to oxygen flow ratio (D) are also found to have significant effects on surface roughness while argon to oxygen flow ratio and operating pressure have less and least impacts on this response, respectively. It can be seen that the coefficient of interaction terms, AC and BC, are comparable to linear terms. Thus, interaction between r.f. power and argon to oxygen flow ratio (AC) and interaction between operating pressure and argon to oxygen flow ratio (BC) have significant effect on surface roughness. A contour plot and a response surface plot for the surface roughness response in terms of the r.f. power and argon to oxygen flow ratio is constructed by using Eq. (4) as shown in Fig. 4. Notice that surface roughness is higher in the region of low r.f. power and carbon doping gas to oxygen flow ratio. The negative signs for the coefficients of r.f. power and carbon doping gas to oxygen flow ratio in the fitted model for surface roughness indicate that the amount of surface roughness increases with decreasing levels of the process factors. The negative signs for the coefficients of interactions among factors mean that an increase in surface roughness is obtained by simultaneous changes of both factors in opposite directions.

The results from quantitative effect analyses on surface roughness can be explained by considering the details of sputtering process along with morphological imaging by SEM. The effect of r.f. power on surface roughness is illustrated in SEM images as shown Fig. 5(a) and (b). It can be seen that the surface morphology of molybdenum oxide thin film is considerably changed as r.f. power is doubled from 100 W to 200 W. For low power one (Fig. 5(a)), it can be seen that the surface is not smooth and contains high density of nanostructure having sharp-end nanorod shape. The length of nanorods is in the range between 0.1 and 0.3 μm and the width is around 20–40 nm. On the contrary, the surface for high power case is considerably smoother with less well-defined smaller nanorods. Similar trends were seen for other pairs of runs with different r.f. powers.

The effect of acetylene to oxygen flow ratio on surface roughness is demonstrated in SEM images as shown Fig. 5(c) and (d). It is evident that the surface morphology of molybdenum oxide thin film is significantly changed as acetylene to oxygen flow ratio is increased from 0:100 (undoped) to 30:70. For undoped one (Fig. 5(c)), it can be seen that the surface is rough and contains high density of sharp-end nanorod shape. The nanorod in this case is relatively larger and longer than those in Fig. 5(a). The length of nanorods is in the range between 0.2 and 0.6 μm and the width is around 20–50 nm. On the contrary, the surface for carbon doped one is smooth with no nanorod. Moreover, it can be noticed that there are some cracks present on the surface of the film in Fig. 5(d). A possible cause of the crack is the difference in thermal expansion coefficient between molybdenum oxide film and the substrate. This only occurs in this case because the heat power generated due to acetylene–oxygen reaction as previously discussed is considerably higher than other cases. Similar trends were seen for other pairs of runs with different carbon doping.

The effects of r.f. power and acetylene to oxygen flow ratio on surface morphology and the formation of nanorods of MoO_x thin film may be explained as followed. In the MoO_x r.f sputtering process, Mo atoms on the target are being knocked-off by ions and then react with oxygen ions

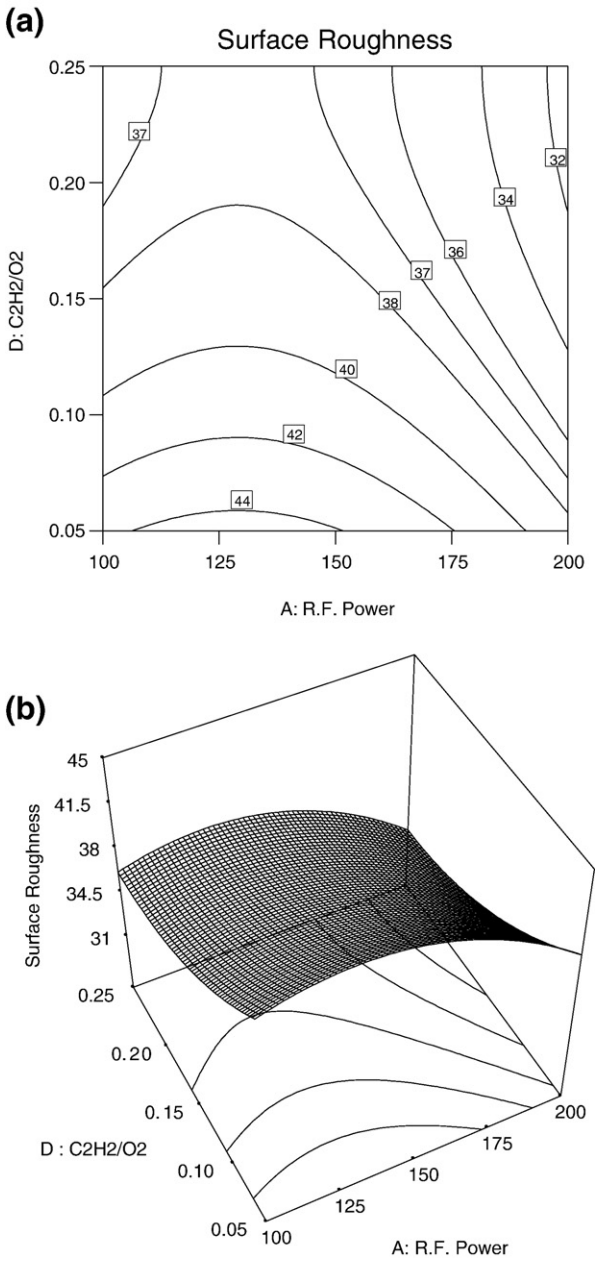

Fig. 4. (a) Contour plot and (b) response surface plot of surface roughness.

in the plasma before arriving at surface of substrates. The nucleation of MoO_x molecules begins and aggregation of following molecules rises with time. The arrangement of deposited molecules is depending on surface energy of deposited molecules and the substrate [14]. Under suitable sputtering conditions including low r.f. power and moderate operating pressure, molybdenum oxide molecules have suitable surface energy such that they tend to nucleate as lines leading to the formation of nanorod and nanobelts structures [6–8].

As r.f. plasma power increases, plasma and substrate temperatures are increased because a fraction of plasma power is converted to heat power and transfers to substrate. In order to verify this assumption, the substrate temperature was measured *in-situ* by a k-type thermocouple attached at the center of substrate holder. The temperature was measured on unheated substrate as a function of plasma power while operating pressure, argon to oxygen and acetylene to oxygen flow ratio were fixed at 0.6 Pa, 40/60 and 90/10, respectively. The steady-state temperature of unheated substrate increased from 105 °C to 160 °C as the plasma power increases from 100 W to 200 W. The result confirms that heat energy is transferred from plasma to substrate and it increases considerably as the plasma power increases.

As the substrate temperature increases, the likelihood of surface to bulk diffusion and surface recrystallization increases, leading to the deformation of nanorod structure and hence a reduction in surface roughness. The effect of acetylene to oxygen flow ratio on surface roughness may be explained by similar mechanism. As acetylene to oxygen flow ratio increases, the temperature of substrate is considerably increased due to combustive reducing reaction as discussed in Eq. (3). In order to prove this hypothesis, the temperature was measured on unheated substrate as a function of acetylene–oxygen flow ratio while plasma power, operating pressure and argon to oxygen flow ratio were fixed at 150 W, 0.6 Pa and 40/60, respectively. The steady-state temperature of unheated substrate increased from 132 °C to 218 °C as the acetylene–oxygen flow ratio increases from 0/100 to 30/70. The result indicates that the combustive reaction significantly increases the substrate temperature. Hence, the increased substrate temperature leads to surface diffusion and coalescence of deposited molecules. It can be noticed that heat generated by the combustive reaction at this acetylene content is so significant that deposited molecules are almost completely coalesced.

Accordingly, the results from response surface analyses for deposition rate and surface roughness indicate that the problem of conflicting responses of deposition rate and surface roughness arises. To overcome the problem of conflicting responses of single response optimization, simultaneous optimization of multi-response variables is used. Since there are a number of operating conditions for the process factors that can be used to maintain all responses within acceptable values, the optimal operating conditions of the process factors should be determined using desirability function. Based on the simultaneous optimization of multi-response variables using RSM, the specific desirability functions are:

$$d_1 = \begin{cases} \left(\dfrac{y_1 - low}{high - low}\right)^r, & low \le y_1 \le high, \\ 0, & \text{otherwise}, \end{cases} \tag{5}$$

and

$$d_2 = \begin{cases} \left(\dfrac{y_2 - low}{high - low}\right)^r, & low \le y_2 \le high, \\ 0, & \text{otherwise}, \end{cases} \tag{6}$$

where d_1 and d_2 are individual desirability functions for both responses whereas *low* and *high* denote the lower and upper limits of the acceptable range. The weight r is assigned to increase or decrease the emphasis given to the specific response in the optimization. For simplicity, $r = 1$ is selected to produce piecewise linear relationships between performance and desirability. For the deposition rate, y_1, the transformation given by Eq. (5) is used with $low = 0.8$ nm/min and $high = 14.7$ nm/min. These limits indicate that the values in the range of 0.8–14.7 nm/min are acceptable. So, values outside that range are not acceptable. For the surface roughness, y_2, the transformation given by Eq. (6) is used with $low = 25$ nm and $high = 55$ nm. These limits indicate that the values in the range of 25–55 nm are acceptable. Then the overall desirability function is defined as follows:

$$D_{12} = (d_1 \times d_2)^{1/2}. \tag{7}$$

Fig. 6 presents a contour plot and a response surface plot of the overall desirability function, D_{12} in terms of the r.f. power and carbon doping gas to oxygen flow ratio. Note that Design-Expert® uses direct search and downhill simplex methods to maximize the overall desirability function. The overall desirability value is higher in the region of low carbon doping gas to oxygen flow ratio. The optimal operating condition is obtained when $A = 150$ W, $B = 0.8$ Pa, $C = 0.59$

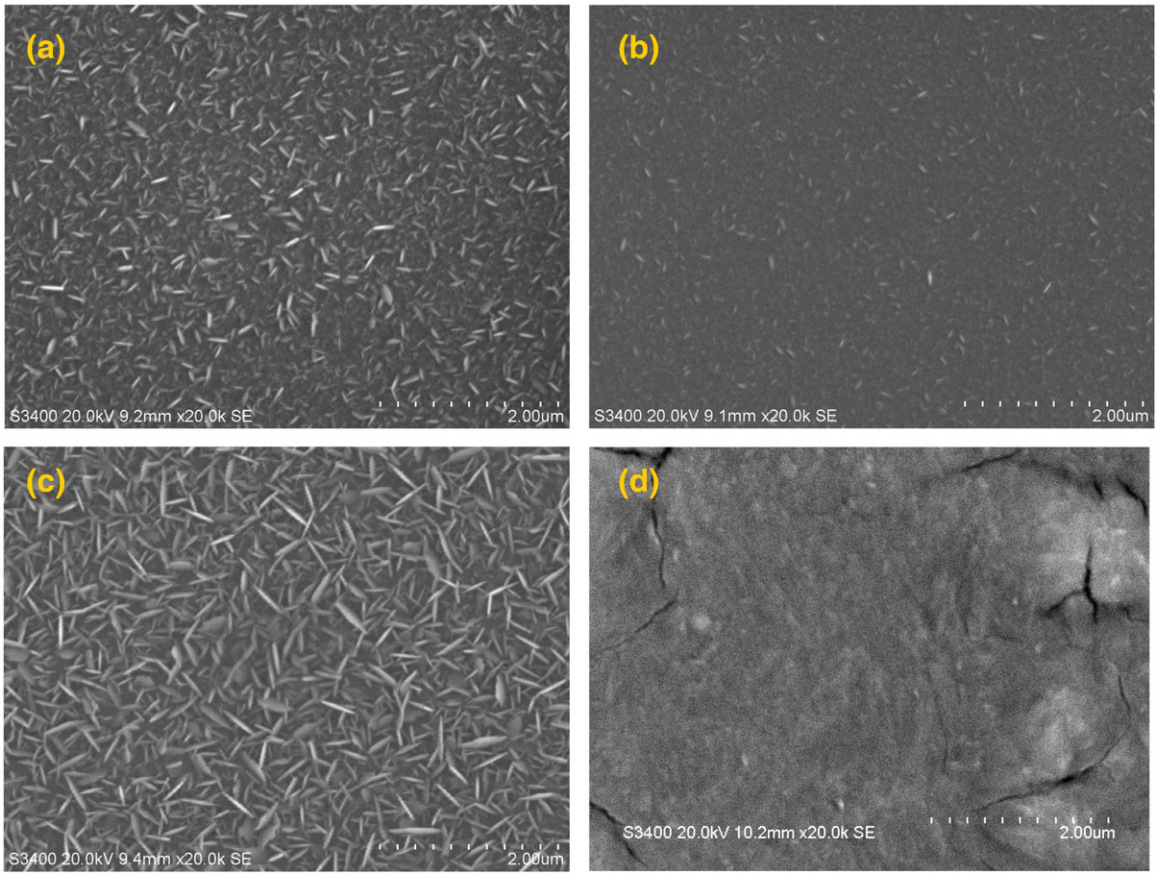

Fig. 5. SEM images of molybdenum oxide thin films (a) trial#2 (low r.f. power of 100 W) (b) trial#10 (high r.f. power of 200 W) (c) trial#29 (low acetylene to oxygen flow ratio of 0:100) and (d) trial#30 (high acetylene to oxygen flow ratio of 30:70).

and $D = 0.08$. This optimal condition produces a maximum deposition rate of 8.4 nm/min, a maximum surface roughness of 41.7 nm, and the overall desirability of approximately 64%. Fig. 6a and b illustrates the contour and response surface plots as function of A and D near the vicinity of optimal setting. Only the plots of factors A and D are illustrated because factors A and D are statistically significant while factors B and C are not according to the ANOVA analysis. It should be noted that the optimal condition does not coincide with any designed experiment. Ability to project an optimal condition beyond original set of experiments is an obvious advantage of response model and RSM analysis.

It can be noticed from Table 1 that the experimental results from trial#30, in which average deposition rate is 9.05 nm/min and average surface roughness is 42.12, are better than the optimum results from the model in term of both deposition rate and overall desirability. This seems to be a contradiction. However, it is in fact not surprising that some observations from experimental designed results are higher or lower than the optimal solution from RSM analysis. Such an observation is regarded as an irregular point that is significantly deviated from prediction of the empirical model. The irregular point can often occur due to several reasons including process variation within experimental runs. This kind of situation has been reported in several literatures [10,21,22]. In this case, trial#30 can be identified as an irregular point for deposition rate with high confidence because the empirical model for deposition rate has high correlation coefficient (R^2 close to 1).

Practically, it is recommended to confirm the optimal operating condition by conducting a confirmation experiment at the optimal operating condition. The confirmation experiment is used to verify whether the predicted response based on the regression model lies within the confidence interval or not. Twenty-five samples were conducted at this condition. From the confirmation runs, the average and standard deviation of deposition rate and surface roughness are 8.26 nm/min, 0.61 nm/min, 42.94 nm, and 3.57 nm, respectively. The 95% confidence interval (CI) for the predicted mean response at the optimal operating condition is given by [24]:

$$CI = \bar{y} \pm 2.064\left(\frac{s}{\sqrt{n}}\right) \tag{8}$$

where $\bar{y}$ represents mean response obtained from confirmation runs, s is sample standard deviation of response obtained from confirmation runs, and n is number of samples or confirmation runs. Thus, 95% confidence interval for the mean response of deposition rate is given by:

$$CI_{DR} = 8.26 \pm 2.064\left(\frac{0.61}{\sqrt{25}}\right)$$
$$= 8.26 \pm 0.25 = (8.01, 8.51)$$

Similarly, 95% confidence interval for the mean response of surface roughness is given by:

$$CI_{SR} = 42.94 \pm 2.064\left(\frac{3.57}{\sqrt{25}}\right)$$
$$= 42.94 \pm 1.47 = (41.47, 44.41)$$

Remind that the predicted responses of deposition rate and surface roughness at the optimal operating condition are 8.4 nm/min and 41.7 nm, respectively. Thus, both predicted responses of deposition rate and surface roughness lie within the 95% confidence interval. This illustrates that the predicted model for the surface roughness is valid and sound.

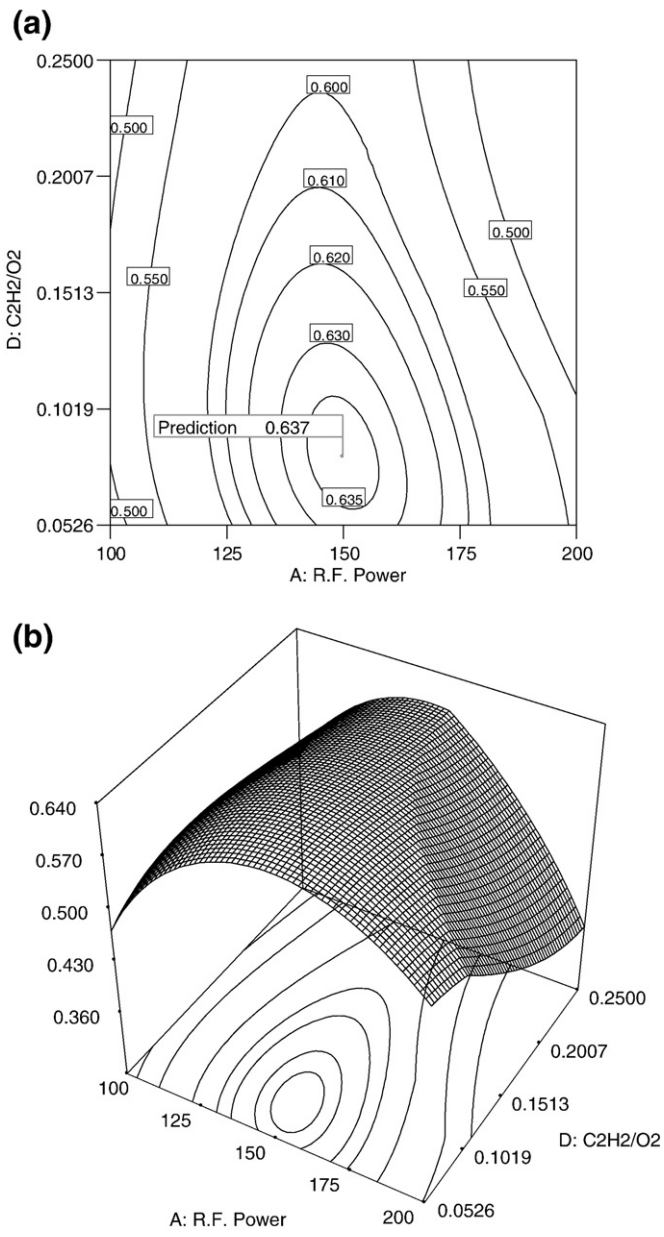

Fig. 6. (a) Contour plot and (b) response surface plot of the overall desirability function.

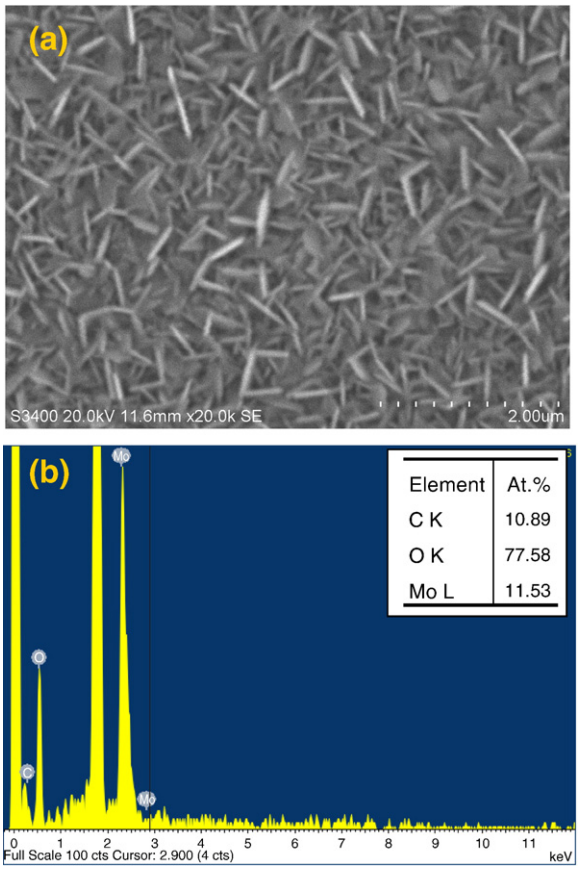

Fig. 7. (a) SEM image and (b) EDX spectrum of molybdenum oxide thin films deposited under optimal condition (r.f. power of 150 W, operating pressure of 0.8 Pa, argon to oxygen flow ratio of 0.59, and acetylene–oxygen flow ratio of 0.08).

The MoO_x thin film prepared under the optimal condition were also examined for surface morphology and chemical composition. The SEM image and EDX spectrum of an optimized MoO_x thin film prepared under this condition is shown in Fig. 7. It can be seen that nanorods are formed under this optimum condition. The nanorod in this case is relatively larger and longer than those in Fig. 5(a) and (c). The length of nanorods is in the range between 0.4 and 0.8 μm and the width is around 20–60 nm. Thus, this condition is suitable for nanorod formation with moderate dimension. From EDX spectra, the carbon content of the film is around 10.9%, which is lower than condition in Fig. 3(b) and (d) but higher than Fig. 3(a) and (c). The result is expected because r.f. power is medium and acetylene–oxygen flow ratio is moderately low under this optimum condition.

Consequently, the results agree well with the predicted model with satisfactory statistical variations. Therefore, optimization using RSM with desirability function has been successfully applied to characterize and control the basic properties of sputtered molybdenum oxide thin film coating. The optimal condition gives process improvement in terms of process throughput with optimal deposition rate and film quality with most favorable surface roughness. In the future, it will be used to optimize other properties including optical, electrical and gas-sensing properties of sputtered molybdenum oxide thin film.

4. Conclusions

In conclusion, we have systematically studied carbon doped MoO_x thin film based on CCD experiment for four controllable factors including r.f. power, operating pressure, argon to oxygen flow ratio, and carbon doping gas to oxygen flow ratio to simultaneously maximize the deposition rate and surface roughness of carbon doped MoO_x thin film coating by RSM with desirability function. The deposition rate and surface roughness can be well described by second order models of these four process factors. From RSM analysis with desirability function, the optimal operating condition for carbon doped MoO_x thin film coating is obtained at r.f. power of 150 W, operating pressure of 0.8 Pa, argon to oxygen flow ratio of 0.59, and carbon doping gas flow ratio of 0.08. This condition produces a maximum deposition rate of 8.4 nm/min, a maximum surface roughness of 41.7 nm and the overall desirability of approximately 64%.

Acknowledgement

The authors would like to thank Khon Kaen University for financial support for the research connected with this paper under grant number 510212002.

References

[1] M. Ferroni, V. Guidi, G. Martinelli, M. Sacerdoti, P. Nelli, G. Sberveglieri, Sens. Actuators B48 (1998) 285.
[2] K. Galatsis, Y.X. Li, W. Wlodarski, K. Kalantar-zadeh, Sens. Actuators B77 (2001) 478.
[3] K. Prasad, P.I. Gouma, D.J. Kubinski, J.H. Visser, R.E. Soltis, P.J. Schmitz, Thin Solid Films 436 (2003) 46.
[4] C. Imawan, H. Steffes, F. Solzbacher, E. Obermeier, Sens. Actuators B78 (2001) 119.
[5] K. Galatsis, Y.X. Li, W. Wlodarski, E. Comini, G. Faglia, G. Sberveglieri, Sens. Actuators B77 (2001) 472.
[6] Y.B. Li, Y. Bando, D. Golberg, K. Kurashima, Appl. Phys. Lett. 81 (2002) 5048.
[7] E. Comini, L. Yubao, Y. Brando, G. Sberveglieri, Chem. Phys. Lett. 407 (2005) 368.
[8] T. Siciliano, A. Teporea, E. Filippoa, G. Micocci, M. Tepore, Mater. Chem. Phys. 114 (2009) 687.
[9] A. Wisitsoraat, A. Tuantranont, V. Patthanasettakul, T. Lomas, J. Nanosci. Nanotechnol. 9 (2009) 897.
[10] O. Keles, G. Aykac, O.T. Inal, Surf. Coat. Technol. 172 (2003) 166.
[11] D.C. Montgomery, Design and Analysis of Experiments, Sixth Edition, John Wiley & Sons, 2005.
[12] G. Derringer, R. Suich, J. Qual. Technol. 12 (4) (1980) 214.
[13] M.J. Anderson, P.J. Whitcomb, RSM Simplified: Optimizing Processes Using Response Surface Methods for Design of Experiments, Productivity Press, 2005.
[14] S.R. Morrison, The Chemical Physics of Surfaces, Plenum Press, 1992.
[15] K. Tsuchiy, T. Kitagaw, Y. Uetsuji, E. Nakamachi, JSME Int. J. Ser. A 49 (2006) 201.
[16] J. Adamczyk, N. Horny, A. Tricoteaux, P.-Y. Jouan, M. Zadam, Appl. Surf. Sci. 254 (2008) 1744.
[17] M. Akiyama, C.-N. Xu, K. Nonaka, K. Shobu, T. Watanabe, Thin Solid Films 315 (1998) 62.
[18] Y. Deng, J.D. Fowlkes, P.D. Rack, J.M. Fitz-Gerald, Opt. Mater. 29 (2006) 183.
[19] K. Hinkelmann, O. Kempthorne, "Design and Analysis of Experiments: Advanced Experimental Design" Volume 2, John Wiley & Sons, New York, 2005.
[20] E.K. Nyutu, S.T. Suib, Surf. Coat. Technol. 201 (2006) 2741.
[21] S.L. Huang, T.C. Wen, A. Gopalan, Mater. Lett. 55 (2002) 165.
[22] D.C. Montgomery, J.B. Keat, L.A. Perry, J.R. Thompson, W.S. Messina, Robot. Comput.-Integr. Manuf. 16 (2000) 55.
[23] A. Laskin, H. Wang, Chem. Phys. Lett. 303 (1999) 43.
[24] D.C. Montgomery, G.C. Runger, Applied Statistics and Probability for Engineers, 2nd edition, John Wiley & Sons, New York, 1998.